Note

Feng-Yang Hsieh

1 CWoLa

The Classification Without Labels (CWoLa) is a weakly supervised learning method. The CWoLa approach trains a model to discriminate the mixed samples, which are mixtures of the original signal and background samples. The optimal classifier in the CWoLa approach is also the optimal classifier in the traditional fully supervised case where all label information is available. This section utilizes the CWoLa approach to train classifiers on di-Higgs samples.

1.1 Sample

This exercise's signal corresponds to the resonant Higgs boson pairs production in the four-b quarks channel. These Higgs boson pairs are produced via gluon-gluon fusion in the two Higgs doublet model (2HDM). The Higgs boson h ($m_h = 125$ GeV) pair is produced by the heavy CP-even scalar H with mass m_H ranging from 300 GeV to 1200 GeV. The background consists of QCD multi-jet events.

The CWoLa training samples M_1 and M_2 are the mixtures of the signal and background samples. The probability distribution of the mixed sample is a combination of the signal $p_s(x)$ and background $p_B(x)$ distributions:

$$p_{M_1}(x) = f_1 p_S(x) + (1 - f_1) p_B(x)$$
$$p_{M_2}(x) = f_2 p_S(x) + (1 - f_2) p_B(x)$$

(1)

where f_1, f_2 are the signal fractions, and x represents the observables used for the classification task.

DNN and SPANet network architectures are considered in this exercise. For DNN, the input features are summarised in Table 1, consisting of 16 variables. For SPANet, the input features are a list of final jets, each represented by their 4-momentum (p_T, η, ϕ, M) and a boolean b-tag.

Table 1: Input variables used to train the dense neural network.

Reconstructed objects	Variables used for training	#
Higgs candidate	$(p_{\mathrm{T}}, \eta, \phi, m)$	8
Subjets	$\Delta R(j_1, j_2)$	2
b-tagging	Boolean for $j_i \in h_{1,2}^{\mathrm{cand}}$	4
Di-Higgs system	$p_{\mathrm{T}}^{hh}, m_{hh}$	2

1.2 Result

The CWoLa training utilizes samples with different signal fractions f_1, f_2 to train the classifiers. The results of CWoLa training are shown in Figure 1 with different signal fractions. When f_1 is far from 0.5, the results tend to approach those of the fully supervised case.
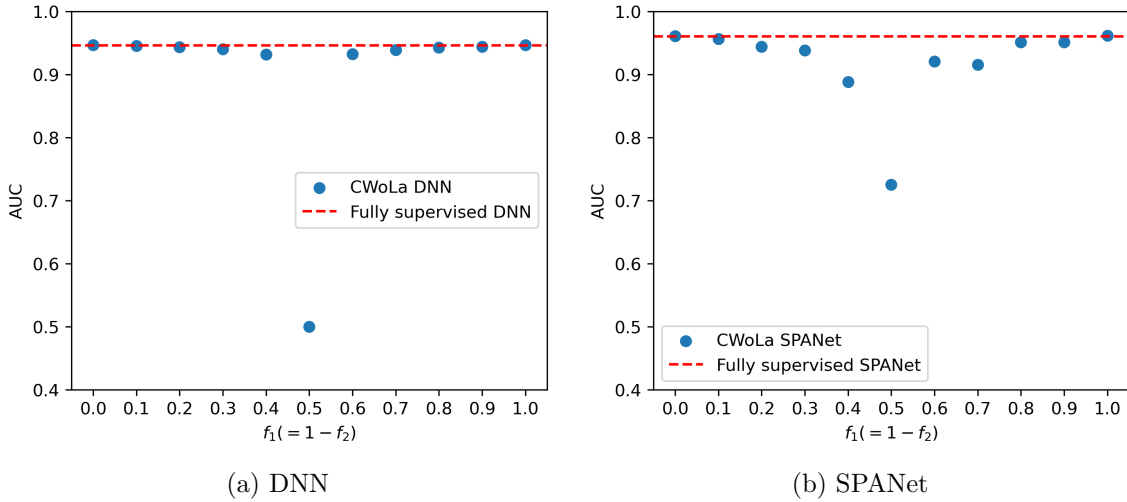

(a) DNN
(b) SPANet

Figure 1: The AUC of CWoLa training as a function of the signal fraction f_1. For simplicity, we set signal fraction f_2 equal to $1 - f_1$. The horizontal dashed line indicates the fully-supervised AUC.

When $f_1 = 0.5$ the mixed sample M_1 and M_2 have identical distributions, so the classifier can not learn anything in this case. In the case of DNN, the AUC is 0.5, as expected. However, for SPANet, the AUC is more than 0.7.

This is because SPANet is trained on both pairing and classification tasks simultaneously. The pairing part introduces some asymmetries between signal and background samples, leading to the AUC that deviates from 0.5.

To investigate the effect of the pairing task on SPANet's performance, the weight of the

pairing component is set to zero, meaning that SPANet focuses solely on the classification task. Figure 2 shows the SPANet training results without pairing task. As expected, the AUC is close to 0.5 when $f_1 = 0.5$.
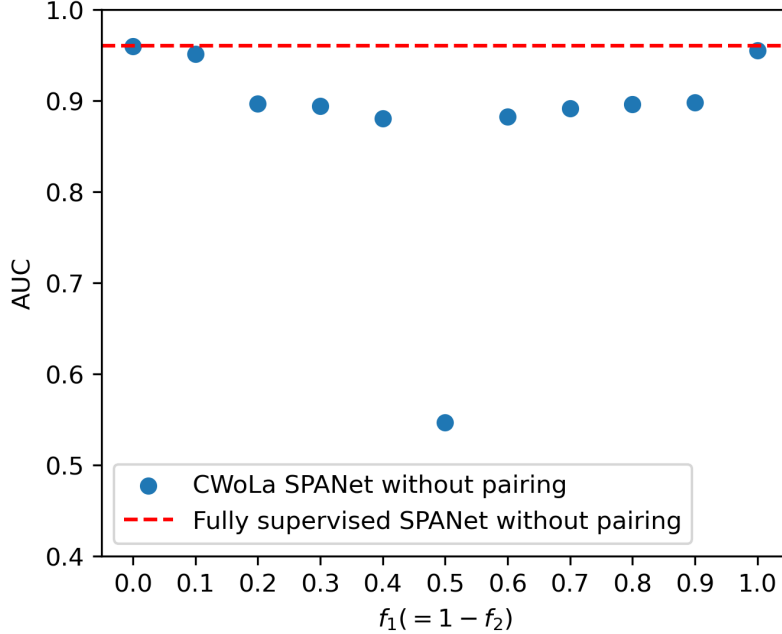

Figure 2: The AUC of CWoLa SPANet training as a function of the signal fraction f_1. For simplicity, we set signal fraction f_2 equal to $1 - f_1$. Here, SPANet is trained on the classification task only.

2   CWoLa hunting

The CWoLa hunting approach considers a variable m_{res}. For background, the m_{res} distribution is smooth while signal m_{res} distribution is expected to be localized near some m_0. Consequently, this variable could be used to create two mixed samples. Additional features that are uncorrelated with m_{res} can be used for training a classifier.

2.1   Sample

The signal is the resonant Higgs boson pairs production in the four-b quarks channel. In this section, the Higgs boson pair is produced by the heavy CP-even scalar H with mass $m_H = 500$ GeV or $m_H = 1000$ GeV. The background consists of QCD multi-jet events. The basic requirement is the "four-tag cut," which requires at least four b-tagged $R = 0.4$ anti-k_t

jets with $p_\mathrm{T} > 40$ GeV and $|\eta| < 2.5$. Only the events passing the four-tag cut are used in the following analysis.

The CWoLa hunting approach utilizes the signal and sideband regions to create the mixed training sample. The di-Higgs system's total invariant mass m_{hh} is utilized to determine the signal and sideband region. This quantity is computed from the four b-jets with the highest transverse momentum. Figure 3 presents the m_{hh} distribution of signal and background samples. Table 2 summarizes the signal and sideband regions. These signal and sideband regions are chosen such that the corresponding cross-sections are closed.
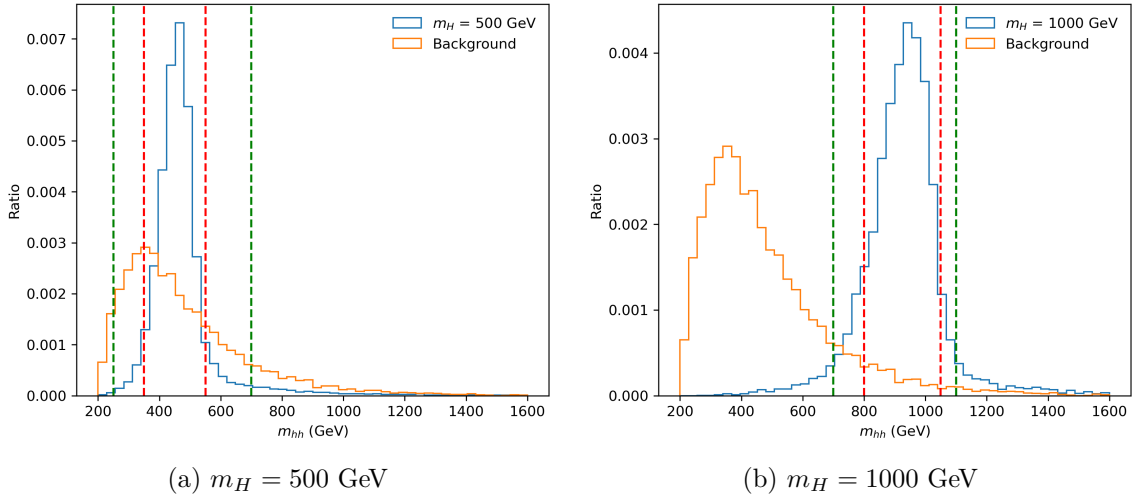

(a) $m_H = 500$ GeV   (b) $m_H = 1000$ GeV

Figure 3: The totoal invriant mass m_{hh} distribution of signal and background samples. The signal region is between the red dashed lines. The sideband region is between the green dashed lines and excludes the signal region.

Table 2: The signal and sideband regions with different resonant samples. The unit is GeV.

m_H	Signal	Sideband
500	$[350, 550]$	$[250, 350] \cup [550, 700]$
1000	$[800, 1050]$	$[700, 800] \cup [1050, 1100]$

Table 3 is the cutflow table of the selection cuts. The number of events used in mixed training samples could be computed from these cross-sections. The training sample size is presented in Table 4.

Consider the DNN CWoLa classifier. The Higgs candidates are reconstructed by the min-ΔR pairing method. In the min-ΔR method, the four b-tagged jets with the highest p_T are used to form the two Higgs boson candidates. The min-ΔR method selects the pairing

Table 3: The cross sections for the di-Higgs signal and background processes at different selection cuts.

| m_H (GeV) | | Cross section (fb) | | S/B | $\mathcal{L} = 139 \text{ fb}^{-1}$ |
		Signal	Background		$S/\sqrt{B}$
500	Four tag	3.64	6.03e+03	6.03e-04	0.553
	Signal region	3.13	2.57e+03	1.22e-03	0.727
	Sideband region	0.35	2.36e+03	1.50e-04	0.086
1000	Four tag	0.081	6.03e+03	1.34e-05	0.0123
	Signal region	0.063	3.32e+02	1.90e-04	0.0408
	Sideband region	0.010	3.19e+02	3.03e-05	0.0064

Table 4: The training sample size for the mixed sample. The luminosity is $\mathcal{L} = 78 \text{ fb}^{-1}$ because the generated samples are not enough for now.

| m_H (GeV) | Mixed sample | True label | |
		Signal	Background
500	M_1	244	200k
	M_2	28	184k
1000	M_1	5	26k
	M_2	1	25k

configuration in which the higher-p_T jet pair has the smallest ΔR separation. The input features are similar to the previous case (Table 1), but the b-tagging information and the di-Higgs system's total invariant mass are excluded. For min-ΔR pairing, it only uses the b-tagged jets. Total invariant mass is already used to determine the signal and sideband region.

2.2 Training results

Table 5 presents the DNN classification training results. These numbers are evaluated from the pure samples, which consist of 5k signal events and 5k background events. The training datasets with and without signal events have similar results. This suggests that the DNN fails to distinguish the signal and background samples but learns the difference between the signal and sideband region. Moreover, the results also imply the input features may correlate to the total invariant mass of the di-Higgs system.

Table 5: The CWoLa DNN training results. ACC is the best accuracy and AUC is the area under the ROC curve. The average and standard deviation of 10 training are presented.

| m_H (GeV)		ACC	AUC
500	With signal	0.708 ± 0.002	0.770 ± 0.007
	No signal	0.705 ± 0.003	0.769 ± 0.009
1000	With signal	0.868 ± 0.024	0.925 ± 0.023
	No signal	0.850 ± 0.033	0.909 ± 0.026

Figure 4 shows the signal score distributions. Even though the signal scores are very different for signal and background distributions, the difference probably stems from the m_{hh} distribution.

There are two issues:

- The input features might correlated to the observables used to determine the signal and sideband region. We need to construct other independent input variables.

- The signal fraction is too low. It is hard to learn something about signal events.

2.3 Correlation matrix

The results in Section 2.2 imply that the di-Higgs system's total invariant mass is not independent of other input features. To find the variables that are highly dependent on
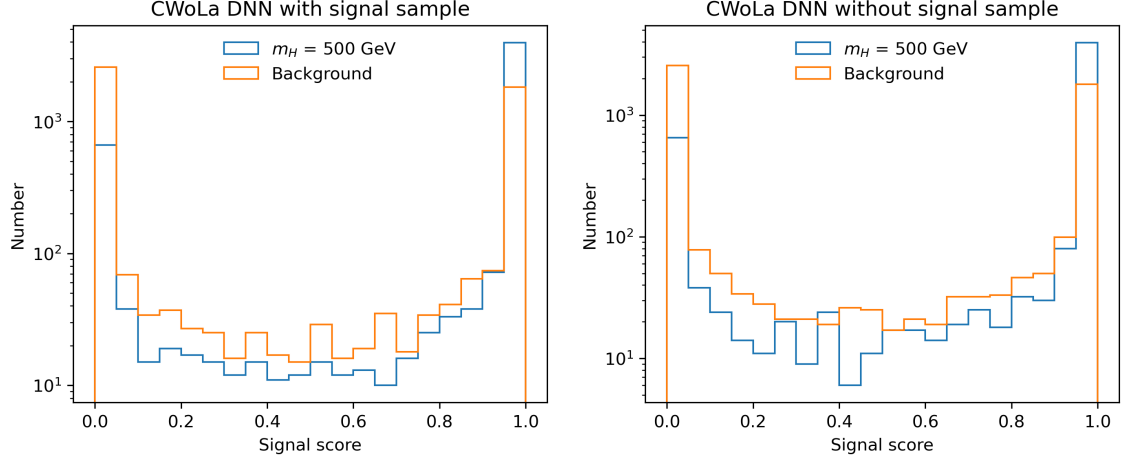
(a) $m_H = 500$ GeV
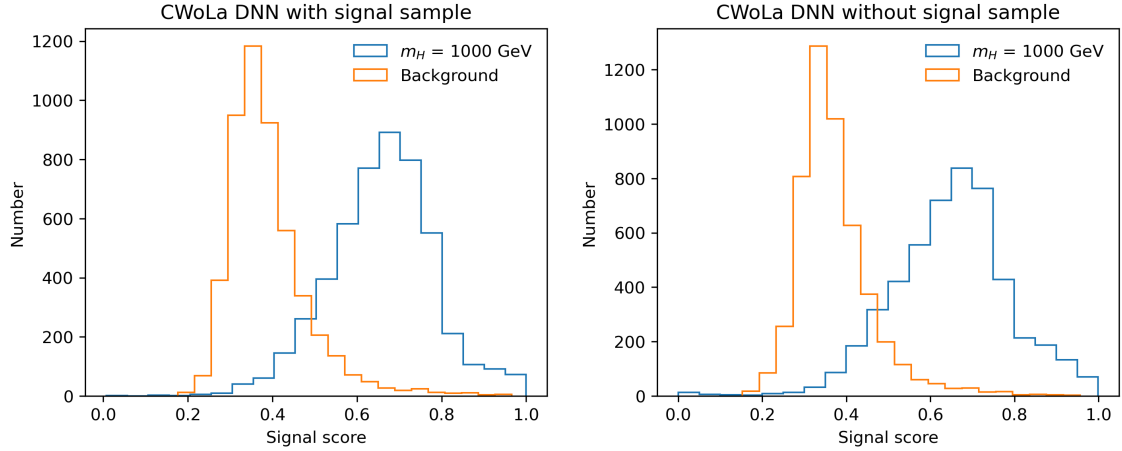
(b) $m_H = 1000$ GeV

Figure 4: The signal score distributions. We apply the CWoLa DNN on pure samples to obtain the signal score distributions.

the total invariant mass, the correlation coefficients are computed among these variables. Figure 5 and 6 are correlation coefficients on the 500 GeV and 1000 GeV cases, respectively.
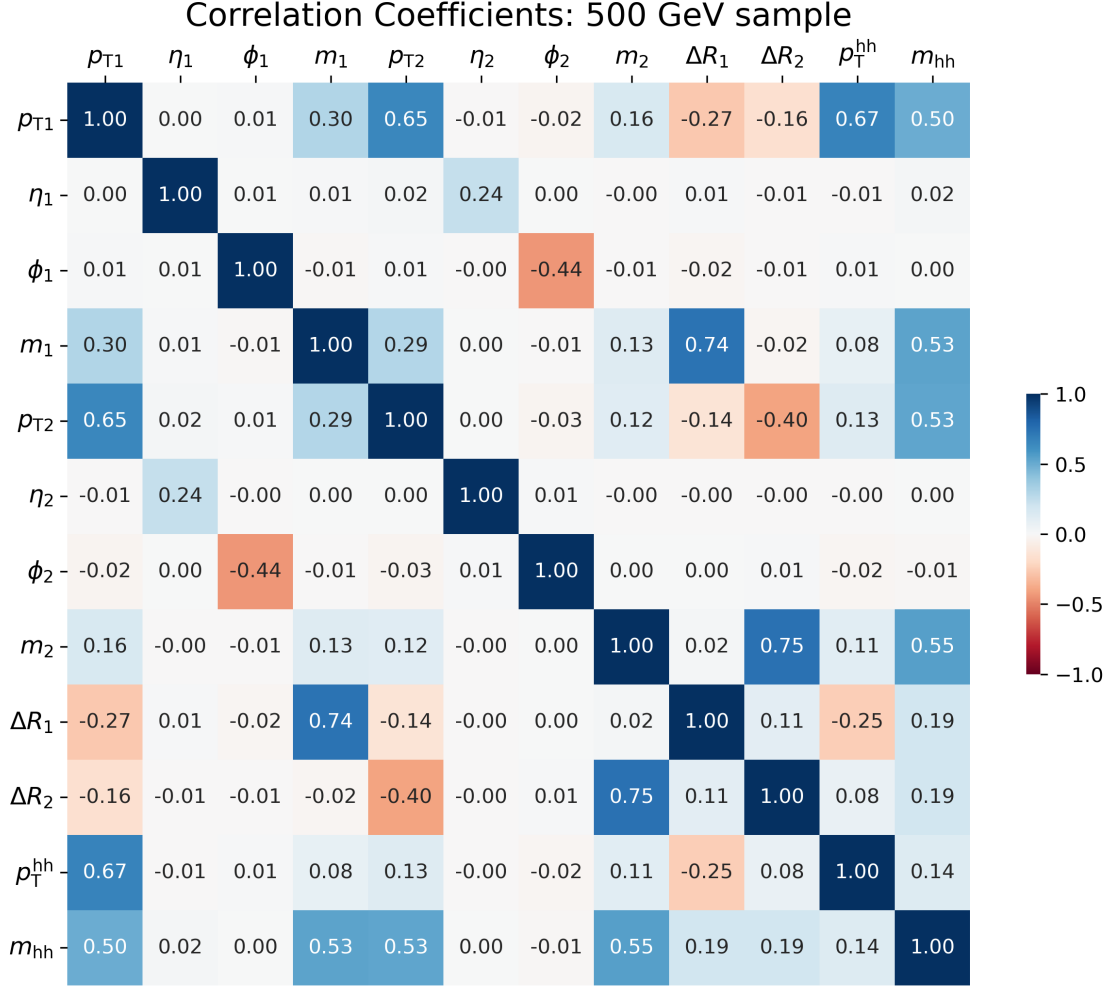

Figure 5: The correlation coefficients among different variables, which are computed from 500 GeV testing sample, which consists of 5k signal and 5k background.

The results show that the transverse momentum p_{T} and the invariant mass m of Higgs candidates are highly correlated to the total invariant mass. Figure 7 shows the scatter plots of the transverse momentum of the leading Higgs candidate and the total invariant mass m_{hh}. These plots also explain why the DNN only trained on background samples can also distinguish the signal and background events, because the background distribution in the signal and sideband regions are different.
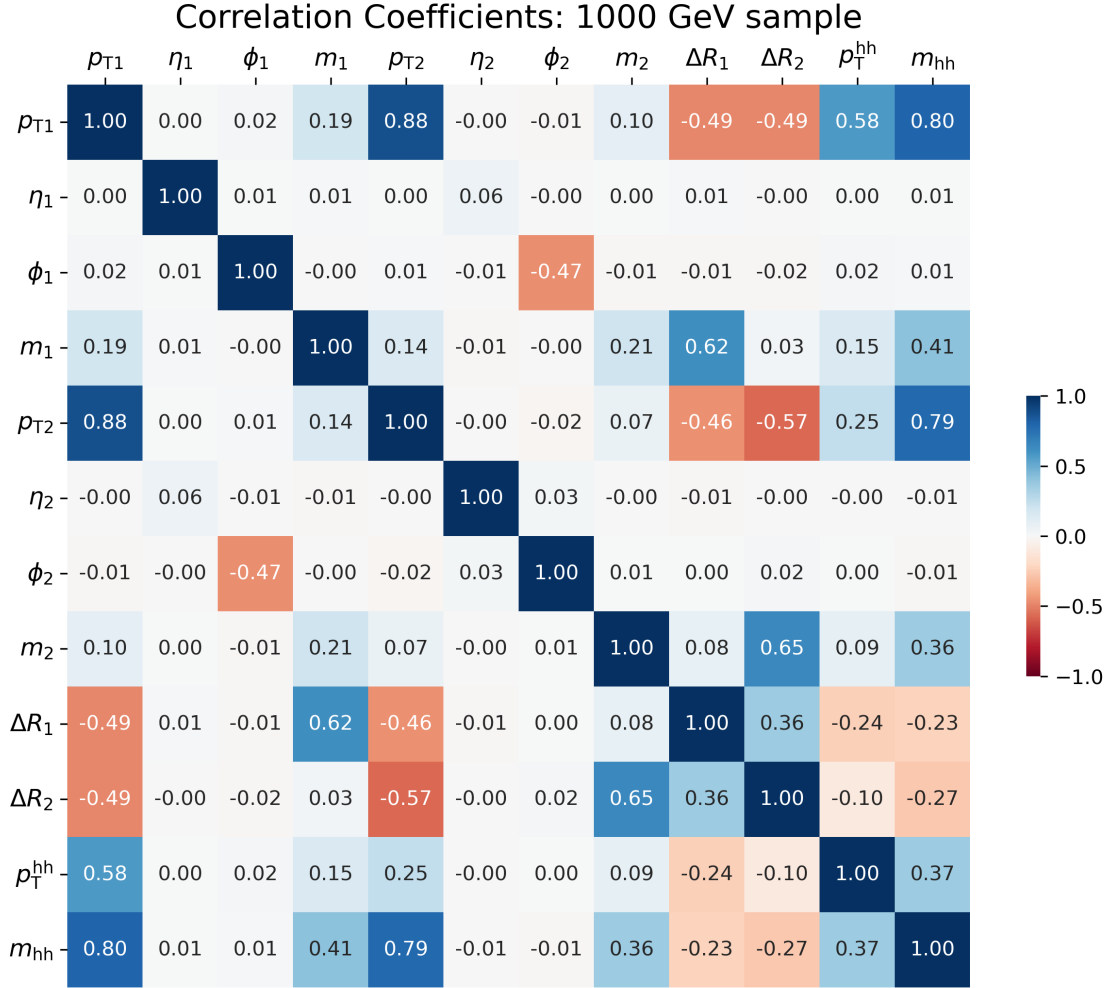
Figure 6: The correlation coefficients among different variables, which are computed from 1000 GeV testing sample, which consists of 5k signal and 5k background.
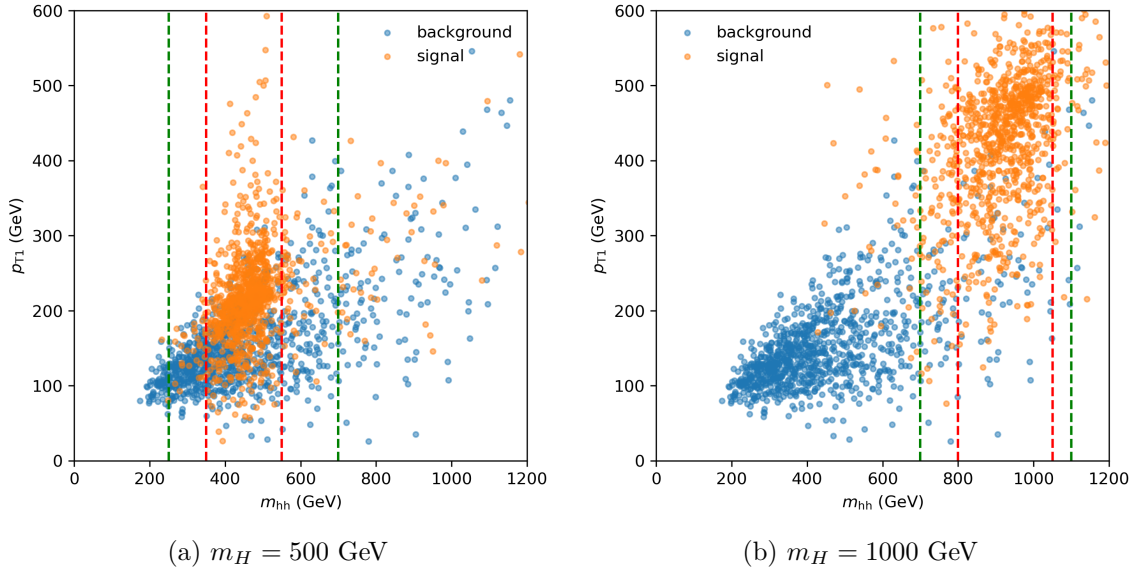
(a) $m_H = 500$ GeV (b) $m_H = 1000$ GeV

Figure 7: The scatter plots of the transverse momentum of leading Higgs candidate p_{T1} and total invariant mass m_{hh} distribution. The signal region is between the red dashed lines. The sideband region is between the green dashed lines and excludes the signal region.

3 Physical data augmentation

The physical augmentations are inspired by Reference [1], which considers the rotation and smearing augmentations. These augmentations reflect both the symmetries in the physical event and the experimental resolution of the detector.

3.1 Original training data

The signal is the resonant Higgs boson pairs production in the four-b quarks channel. In this section, the Higgs boson pair is produced by the heavy CP-even scalar H with mass $m_H = 500$ GeV. The background consists of QCD multi-jet events. The basic requirement is the "four-tag cut," which requires at least four b-tagged $R = 0.4$ anti-k_t jets with $p_T > 40$ GeV and $|\eta| < 2.5$. Only the events passing the four-tag cut are used in the following analysis.

The training samples consist of 50k signal events and 50k background events and the testing samples consist of 5k signal events and 5k background events.

The Higgs candidates are reconstructed by the min-ΔR pairing method. The input features are similar to the previous case (Table 1), but the b-tagging information is excluded.

3.2 Physical augmentation

We consider three different physical augmentations.

1. Azimuthal rotation: The whole final state is rotated by an angle ϕ randomly sampled from $[0, 2\pi]$.

2. $\eta - \phi$ smearing: The (η, ϕ) coordinate of Higgs candidates are resampled according to a Normal distribution centered on the original coordinate and with a standard deviation inversely proportional to the p_T

$$\eta' \sim \mathcal{N}\left(\eta, \frac{\Lambda}{p_T}\right), \quad \phi' \sim \mathcal{N}\left(\phi, \frac{\Lambda}{p_T}\right) \tag{2}$$

where η', ϕ' are the augmented coordinate, p_T is the transverse momentum of the Higgs candidate, and the smearing scale is set to be $\Lambda = 10$ GeV.

3. p_T smearing: The p_T of Higgs candidates are resampled according to

$$p_T' \sim \mathcal{N}\left(p_T, f(p_T)\right), \quad f(p_T) = \sqrt{0.052p_T^2 + 1.502p_T} \tag{3}$$

where p_T' is the augmented transverse momentum, $f(p_T)$ is the energy smearing applied by `Delphes` (the p_T's are normalised by 1 GeV).

Figure 8, 9 and 10 are the distributions before and after the augmentation. For the $\eta - \phi$ smearing, the distributions are similar for both cases. For p_T smearing, it makes the peak broaden and the transverse momentum distribution looks smoother.

For each type of augmentation, we test "n times augmentation" with different n. The n times augmentation means for one original sample, we generate n augmented samples. Additionally, we test another case that applies all augmentations at the same time.

3.3 Training results

Table 6 presents the DNN classification training results of the original sample. Table 7 are the training results of the augmented samples. For each type of augmentation, they all can improve the ACC by about 4%. The differences among the various augmentation are not significant. The 10-times augmentation has the best results, but the difference between the 5-times and 10-times augmentation is very small. It seems that the performance of this classifier is saturated.
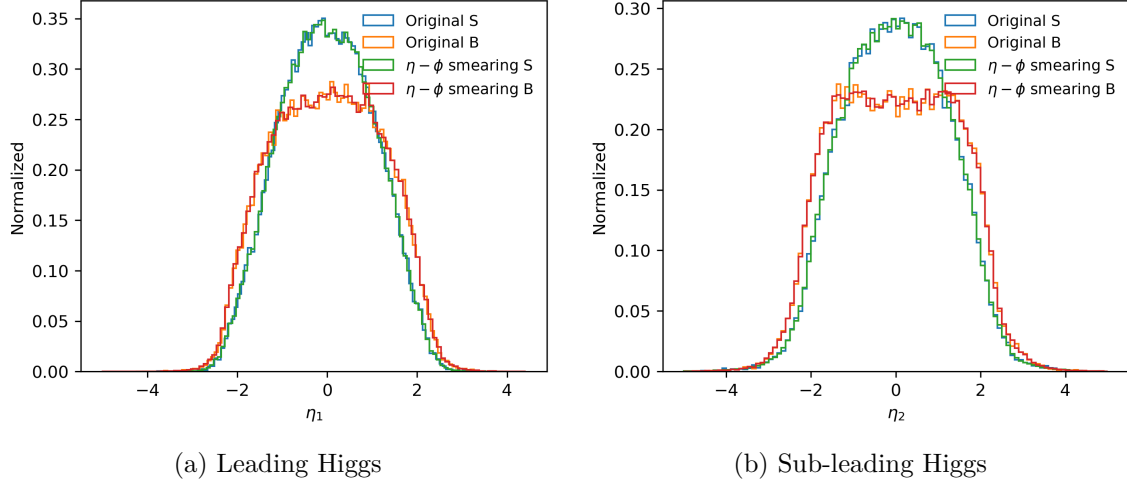
(a) Leading Higgs
(b) Sub-leading Higgs

Figure 8: The pseudorapidity distribution before and after the $\eta - \phi$ smearing augmentation. η_1 and η_2 are the pseudorapidities of the leading and the sub-leading Higgs candidate, respectively.

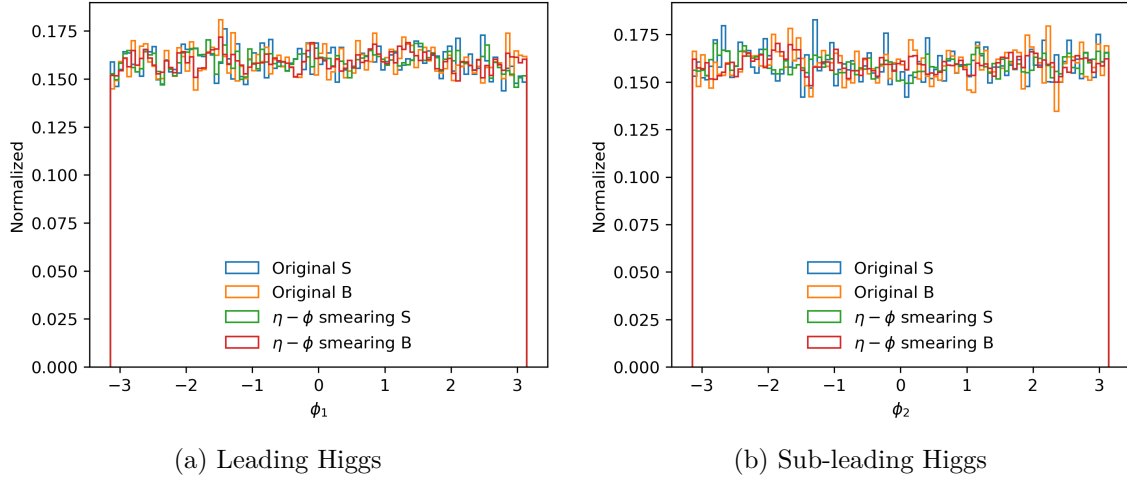(a) Leading Higgs
(b) Sub-leading Higgs

Figure 9: The azimuthal angle distribution before and after the $\eta - \phi$ smearing augmentation. ϕ_1 and ϕ_2 are the azimuthal angles of the leading and the sub-leading Higgs candidate, respectively.

Table 6: The training results of original samples. ACC is the best accuracy and AUC is the area under the ROC curve. The average and standard deviation of 10 training are presented.

	Original
ACC	0.845 ± 0.015
AUC	0.917 ± 0.005

(a) Leading Higgs
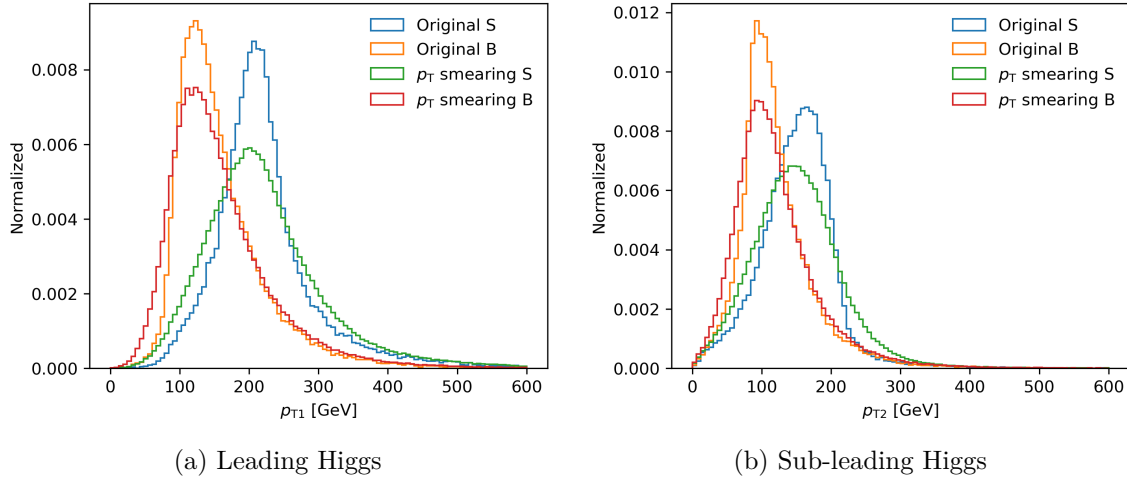
(b) Sub-leading Higgs

Figure 10: The transverse momentum distribution before and after the p_{T} smearing augmentation. $p_{\mathrm{T}1}$ and $p_{\mathrm{T}2}$ are the transverse momentum of the leading and the sub-leading Higgs candidates, respectively.

Table 7: The training results of augmented samples. ACC is the best accuracy and AUC is the area under the ROC curve. The average and standard deviation of 10 training are presented.

		Rotation	$\eta - \phi$ smear	p_{T} smear	All
3 times	ACC	0.880 ± 0.007	0.879 ± 0.010	0.882 ± 0.003	0.875 ± 0.011
	AUC	0.950 ± 0.007	0.949 ± 0.008	0.951 ± 0.003	0.942 ± 0.012
5 times	ACC	0.887 ± 0.002	0.887 ± 0.001	0.890 ± 0.002	0.889 ± 0.003
	AUC	0.955 ± 0.001	0.955 ± 0.001	0.957 ± 0.001	0.956 ± 0.001
10 times	ACC	0.889 ± 0.001	0.889 ± 0.002	0.892 ± 0.002	0.892 ± 0.002
	AUC	0.956 ± 0.001	0.956 ± 0.001	0.958 ± 0.001	0.958 ± 0.000

References

[1] Barry M. Dillon, Luigi Favaro, Friedrich Feiden, Tanmoy Modak, and Tilman Plehn. Anomalies, Representations, and Self-Supervision. 1 2023.